Article ID: 1000-5773(2008)03-0298-07

Two-Dimensional Numerical Simulation of Gas/Liquid Interface Instability*

WANG Tao, BAI Jing-Song, LI Ping

(*Institute of Fluid Physics, CAEP, Mianyang* 621900, *China*)

Abstract: On the basis of multi-fluid volume fraction(VOF) and piecewise parabolic method(PPM), a multi-fluid hydrodynamic program MFPPM(Multi-Fluid Piecewise Parabolic Method) was developed and performed to study the Richtmyer-Meshkov instability of gas/liquid interface. The influences of initial perturbations and grids on the fluid mixing zone(FMZ) were mainly researched when it is accelerated by shock waves, and the FMZ width, bubble and spike height growing with time were presented simultaneously. By comparing the computational results, it shows that the initial perturbations affect the FMZ growth rate extremely, especially at late times. The evolution of spike is similar to the FMZ, the bubble height increases linearly with time basically, and influenced little by initial perturbations, but the configuration is quite different, and as the effect of grid size is.

Key words: multi-fluid hydrodynamic; Richtmyer-Meshkov instability; fluid mixing zone

CLC number: O347; O354 **Document code**: A

1 Introduction

The instability of a material interface under an acceleration of an incident shock was predicted theoretically by Richtmyer in 1960[1]. Ten years later, Meshkov confirmed, experimentally, Richtmyer's prediction[2]. Since then, this interfacial instability is known as the Richtmyer-Meshkov (RM) instability. The RM instability is closely related to the Rayleigh-Taylor(RT) instability[3-5], which is an interfacial instability between two fluids of different densities driven by an external force. RM and RT instabilities share certain common features: the formation and growth of bubbles and spikes. The bubble is the portion of light fluid penetrating into heavy fluid, and the spike is the portion of heavy fluid penetrating into light fluid. Bubbles and spikes grow with time in opposite directions. However, the dynamics of RM and RT instabilities are qualitatively different. The RT interface is unstable only when the external force acts from heavy fluid to light fluid, whereas the RM interface is always unstable whether the shock wave collides with the material interface from the heavy fluid phase to the light fluid phase or vice versa. The presence of shock waves in the RM instability significantly complicates theoretical, numerical, and experimental studies.

Richtmyer-Meshkov instability is of importance in fields ranging from astrophysics to combustion. For example, RM instability is very important to studying of mixing and combustion in scramjet, inertial confinement fusion(ICF) driven by laser. It can also be used to explain some phenomenon of supernovae dynamics in astrophysics. Its later nonlinear evolvement is extremely significant to reveal

* **Received date**: 2007-03-25; **Revised date**: 2007-05-28

Foundation Item: Foundation of China Academy of Engineering Physics(2008B0202011)

Biography: WANG Tao(1979 —), male, master, Major in computational fluid dynamics and instability.
E-mail: wtaoxp@21cn.com

the essence of compressible turbulence. In this study, we presented a detailed numerical study of the gas/liquid RM instability[6-7] and finally gave some qualitative conclusions. In our simulations the gas is air and the liquid is water. As far as know, the papers or reports published about the gas/liquid interface instability were few up to now.

2 Numerical Method

On the basis of volume of fraction (VOF) model[8], we combined the Piecewise Parabolic Method[9] (PPM) with the interface tracking to apply to hydrodynamic Euler equations, and it involved a two-step Lagrange-Remapping algorithm to solve the multi-fluid hydrodynamic problems. The governing equations can be written as follows

$$\begin{cases} \dfrac{\partial \rho}{\partial t} + \dfrac{\partial \rho u_j}{\partial x_j} = 0 \\ \dfrac{\partial \rho u_i}{\partial t} + \dfrac{\partial \rho u_j u_i}{\partial x_j} + \dfrac{\partial p}{\partial x_i} = 0 \\ \dfrac{\partial \rho E}{\partial t} + \dfrac{\partial (\rho u_j E + p u_j)}{\partial x_j} = 0 \\ \dfrac{\partial Y^{(s)}}{\partial t} + u_j \dfrac{\partial Y^{(s)}}{\partial x_j} = 0 \qquad s = 1, 2, \cdots, N-1 \end{cases} \tag{1}$$

Here, i and j represent the three directions of x, y, z respectively, and the same i and j express summation, $\rho, u_k (k = i, j), p$ are density, velocity and pressure of materials, E is the total energy of a unit mass, N is the number of species of media, $Y^{(s)}$ is the volume fraction of s^{th} species and satisfies $\sum Y^{(s)} = 1$. Equation of states is the form of "stiffen gas"

$$p = (\gamma - 1)\rho e - \gamma \pi \tag{2}$$

for gas, γ is the ratio of specific heat, and $\pi = 0$. For liquid and flexible close-grained media described by impact Hugoniot curve, γ is the fitting constant of material. π is the material constant with viscous tensor dimension. Multidimensional problems can be simplified to several one-dimensional ones by dimension splitting method.

In order to capturing the material interface effectively, Two-step Lagrange-Remapping arithmetic is used to solve the Eq. (1). The all calculations are divided into four steps: the first, piecewise parabolic interpolation of physical quantities; the second, solving of approximation Riemann problems; the third, marching solving of Lagrange equations; the fourth, mapping the physical quantities to stationary Euler grid. In the second step, bi-shock approximation method is used to resolve the Riemann problems. In Lagrange step, the physical quantities were achieved in Lagrange coordinates, and they must be remapped to the stationary Euler grid by the fourth step at last. And the calculations for last two steps were referred to Ref. [10].

3 Computational Model and Conditions

The computational model is described as Fig. 1. The zone width of high pressure gas He is 250 mm, the zone width of water is also 250 mm, the width of air zone between He and water is 500 mm. The right of model is connected with atmosphere. The initial conditions are in the

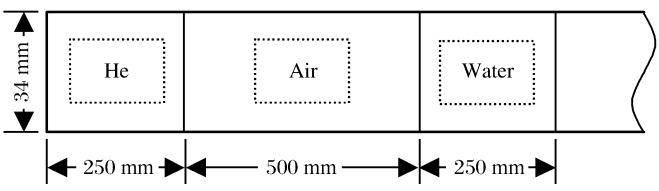


Fig. 1　Computational model

table 1. The interface is impacted by high pressure He gas, and the gravity is negligible.

Table 1 Initial conditions

Material	Pressure/(MPa)	Density/(kg/m^3)	Velocity/(m/s)	γ	π /(MPa)
He	0.25	0.304 2	0.0	1.667	0.0
Air	0.10	1.292 8	0.0	1.4	0.0
Water	0.10	1 000.0	0.0	7.0	387.5

In the calculations, we set four kinds of initial perturbations at the interface of air and water, and the computational domain was divided into 26 zones for parallel calculations (using 26 CPUs), the mesh is square for 100×68 and 200×136 for each zone, the sizes of grids Δ are 0.5 mm (coarse grid) and 0.25 mm (fine grid) respectively. Perturbation 1 is a random perturbation; perturbation 2 is a natural perturbation (The interface is a concave surface from left to right), perturbation 3 is a point perturbation which is a small semicircle penetrating into water in the middle of the interface; perturbation 4 is a combined perturbation which is a small semicircle penetrating into water in the middle of the interface and a cosine beside the semicircle. For the initial perturbations, the amplitude and radius of the semicircle are 2 mm for coarse grid and 1 mm for fine grid respectively.

4 Simulations and Discussion

We studied the RM gas/liquid (Air/Water) interface instability numerically by this instance, the main purpose is researching developing of the FMZ, bubbles and spikes with time, and the effects of different perturbations and grids on the FMZ growth rate and width of bubbles and spikes. When the incident shock collides with the material interface from gas phase (light fluids phase) to liquid phase (heavy fluids phase), it bifurcates into a transmitted shock and a reflected shock. For this case, the left and right boundary are all inflow/outflow conditions, therefore the shock only acts on the interface once. Fig. 2(a)～Fig. 2(l) present a sequence of density images showing the development of interface for perturbation 1 and fine grid. The initial random perturbation can be considered as a superposition of waves with an independent Fourier wavelength. According to the linear theory, the Fourier models of short wavelength grow faster than long wavelength. When entering nonlinear stage, the interface develops bubbles and spikes for nonlinearity (see Fig. 2(d)). And the bubbles will become more blunter, the spikes will become more peaked. The larger bubbles advance faster than smaller ones, finally overtake adjacent smaller neighbors and become more larger (Fig. 2(e)～Fig. 2(l)). This phenomenon is called bubble merger[11].

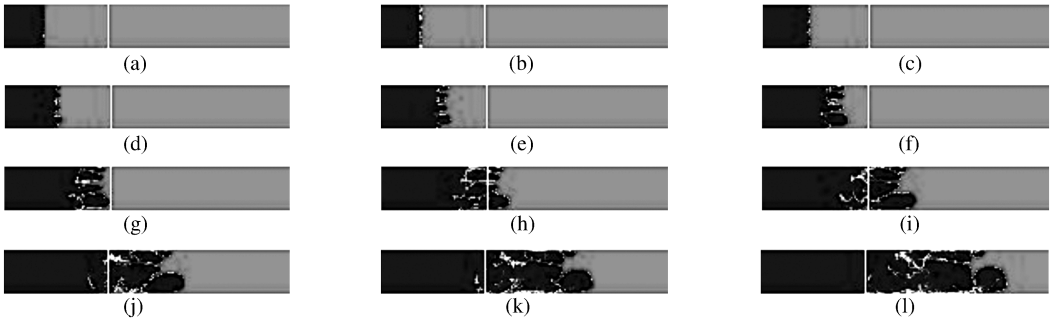


Fig. 2 A sequence of density images showing the development of interface, time interval is 2 ms (The dark part is air and the light part is water)

The air/water interface of different initial perturbations and grid size Δ at one time are presented in Fig. 3. It can be seen clearly that the configurations of FMZ is affected extremely by initial perturbations and grid size, and are quite different for each other; the same as the bubbles and spikes. The perturbation 2 and perturbation 3 can be considered as single models. The bubble may be single (Fig. 3(c) and Fig. 3(e)), or several and bubble merger can occur (Fig. 3(d)). The larger bubbles or spikes grow faster, the reason is that they have a smaller ratio of area to displaced fluid volume, and therefore less drag per unit mass according to Newton's law. The perturbation 1 and perturbation 4 are multi-models with different wavelength, the unstable interface can develop into bubbles and spikes with different sizes, the bubble merger must occur, and the wavelength plays a key role in the evolution of perturbations.

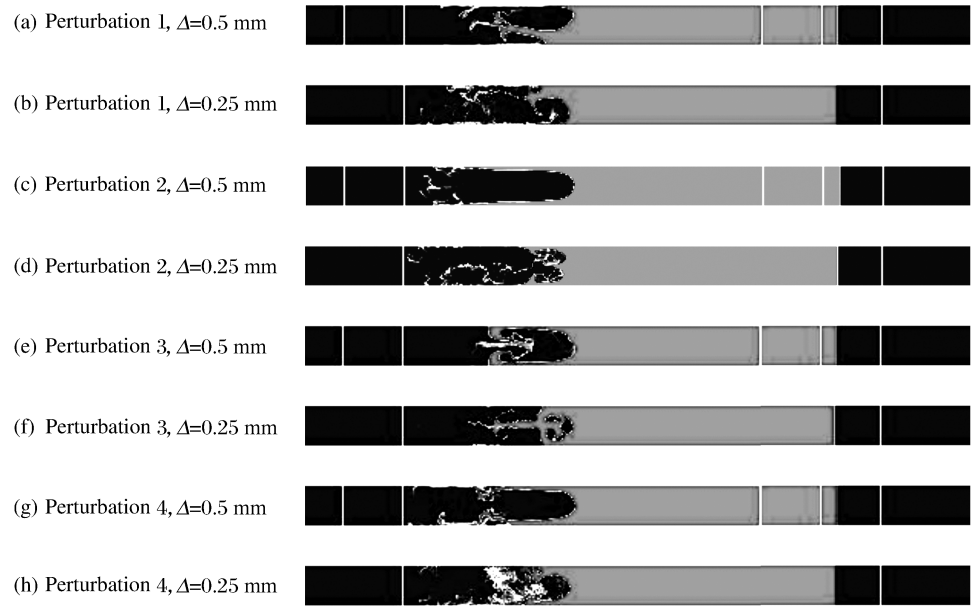
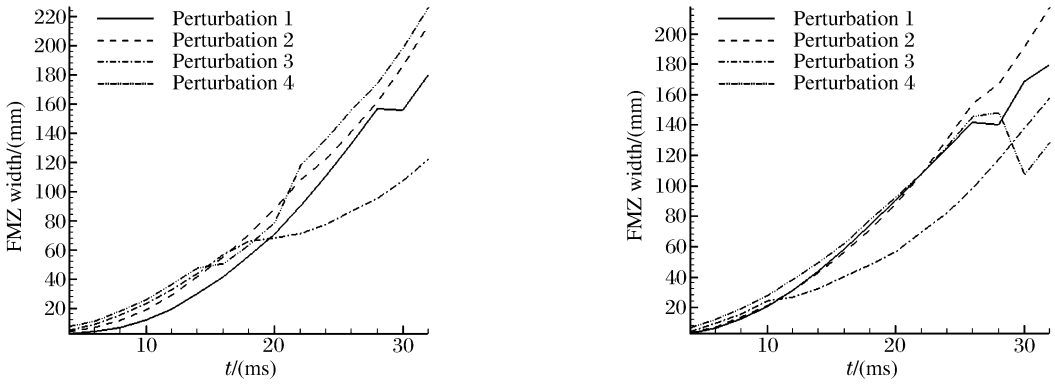


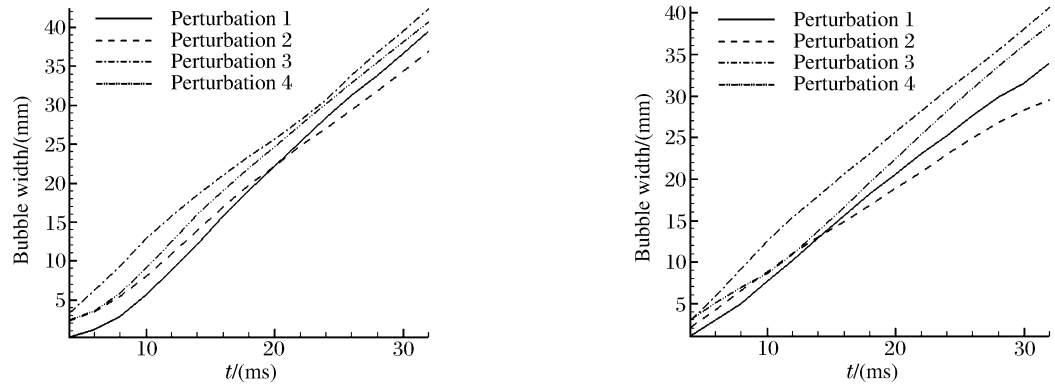
Fig. 3　Configuration of Air/Water interface of different initial perturbations and grid size Δ at one time

In Fig. 4, it gives the width of FMZ vs. time for different initial perturbations (Fig. 4(a) for coarse grid $\Delta=0.5$ mm, Fig. 4(b) for fine grid $\Delta=0.25$ mm). The width of FMZ is increasing with time. It is influenced little at early times, but severely at late times by initial perturbations, for the linearity mainly operates in linear stage, the deformation of interface is less, the perturbation is developing slowly. In the nonlinear stage, the nonlinearity of flow enhances gradually and mainly operates, and the bubbles and spikes grow faster for different wavelength with different velocities. The widths of bubbles and spikes vs. time for different initial perturbations is presented in Fig. 5 and Fig. 6 respectively (Fig. 5(a) and Fig. 6(a) for coarse grid $\Delta=0.5$ mm, Fig. 5(b) and Fig. 6(b) for fine grid $\Delta=0.25$ mm). In the process of developing of the FMZ, the width of bubbles is increasing linearly with time basically, and is influenced little by initial perturbations. Whereas the developing of spikes is too different with bubbles, and similar to FMZ. The width of spikes is influenced little at early times, but extremely at late times by initial perturbations. The FMZ width is the summation of the bubble width and spike width, the spike width is increasing more faster than bubble width with time. The widths of FMZ, bubble, and spike are affected little by grid size, but the configurations are much too different.



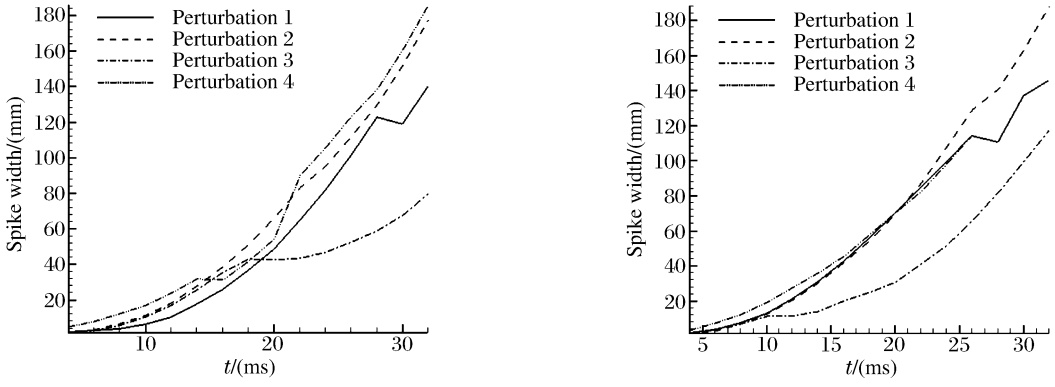
(a) $\Delta=0.5$ mm (b) $\Delta=0.25$ mm

Fig. 4 FMZ width vs. time for different initial perturbations



(a) $\Delta=0.5$ mm (b) $\Delta=0.25$ mm

Fig. 5 Width of bubble vs. time for different initial perturbations



(a) $\Delta=0.5$ mm (b) $\Delta=0.25$ mm

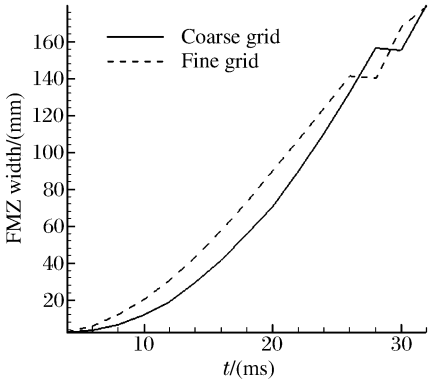
Fig. 6 Width of spike vs. time for different initial perturbations

Here, we defined a proportionality factor λ which is the ratio of the difference of the largest width and smallest width of FMZ, or bubble, or spike to the length of computational model. Table 2 shows

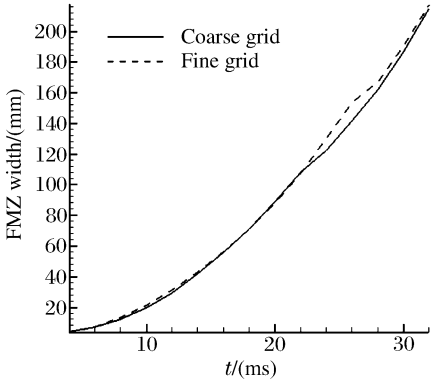
the values of λ. By comparing λ, we can also conclude that the widths of FMZ and spike are affected extremely, and the width of bubble is affected little by initial perturbations, they are all affected little by grid size. The FMZ width vs. time for different grid sizes are presented in Fig. 7. It reveals that the FMZ width is influenced little relatively by grid, whereas the configuration is greatly different as above.

Table 2　The values of λ

	FMZ	Spike	Bubble		FMZ	Spike	Bubble
Coarse grid	10.85%	8.14%	0.41%	Fine grid	11.55%	7.50%	0.86%



(g) Perturbation 1



(h) Perturbation 2

Fig. 7　FMZ width vs. time for different grid sizes Δ

5　Summary

Two-dimensional numerical simulation was performed in order to investigate the RM gas/liquid interface instability, the effects of initial perturbations and grid size on the FMZ by using the multi-fluid PPM method. We can conclude:

(1) The evolution of FMZ is affected extremely by initial perturbations, especially, at late times, but the FMZ width is influenced little at early times. It is similar to the FMZ for the developing of spikes affected by initial perturbations.

(2) The bubbles width is increasing linearly with time basically, and is affected little by initial perturbations.

(3) The widths of FMZ, bubble, spike are affected little by grid size, but the configurations are greatly different each other.

Here, it should be noted that, the viscosity was not considered in our simulations. The instability will result in happening of turbulence mixing ultimately, and the viscosity is of importance and should be considered when studying turbulence. So how and what the viscosity influences the TMZ(Turbulent Mixing Zone) is the future work.

References:

[1] Richtmyer R D. Taylor Instability in Shock Acceleration of Compressible Fluids [J]. Commun Pure Appl Math, 1960, 13: 297-319.

[2] Meshkov E E. Instability of a Shock Wave Accelerated Interface between Two Gases [J]. NASA Tech Trans,

1970,F-13:74.

[3] Rayleigh L. Investigation of the Character of the Equilibrium of an Incompressible Heavy Fluid of Variable Density [J]. Proc Lond Math Soc,1883,14:170-177.

[4] Taylor G I. The Instability of Liquid Surface when Accelerated in a Direction Perpendicular to Their Planes Ⅰ [J]. Proc R Soc London A,1950,201:192-196.

[5] Sharp D H. An Overview of Rayleigh-Taylor Instability [J]. Physica D,1984,12:3-18.

[6] Wang X L,Itoh M,Shi H H,et al. Experimental Study of Rayleigh-Taylor Instability in a Shock Tube Accompanying Cavity Formation [J]. Jpn J Appl Phys,2001,40:6668-6674.

[7] Shi H H,Kishimoto Masami. Fluid Mechanics in the Transient Acceleration of a Liquid Column [J]. Explosion and Shock Waves,2003,23(5):391-397. (in Chinese)
施红辉,岸本薰实. 瞬态加速液柱的流体力学问题研究 [J]. 爆炸与冲击,2003,23(5):391-397.

[8] Hankin K S R. The Euler Equations for Multiphase Compressible Flow in Conservation Form [J]. J Comput Phys, 2001,172: 808-826.

[9] Colella P,Woodward P R. The Piecewise Parabolic Method(PPM) for Gas Dynamical Simulations [J]. J Comput Phys,1984,54:174-201.

[10] Bai J S,Li P,Tan D W. Simulations of the Instabilities Experiments in Stratified Cylindrical Shells [J]. Chinese Physics Letter,2006,23(7):1850-1852.

[11] Alon U,Hecht J,Ofer D,et al. Power Laws and Similarity of Rayleigh-Taylor and Richtmyer-Meshkov Mixing Fronts at All Density Ratios [J]. Phys Rev Lett,1995,74(4):534-537.

二维气/液界面不稳定性数值模拟

王 涛,柏劲松,李 平

(中国工程物理研究院流体物理研究所,四川绵阳 621900)

摘要:以多介质的体积分数方法和三阶PPM(Piecewise Parabolic Method)方法为基础,给出了适用于多介质流体动力学数值模拟的计算方法和程序MFPPM。利用MFPPM程序对在高压气体冲击作用下的气体/液体交界面的Richtmyer-Meshkov(RM)不稳定性及其引起的流体混合现象进行了数值模拟研究。主要研究在不同的初始扰动情况下流体混合区的发展,并细致研究了流体混合区的宽度、气泡和尖钉高度随时间的增长情况及不同初始扰动对它们的影响;同时还研究了网格尺度不同时混合区、气泡以及尖钉的构型和高度的增长情况。通过对计算结果的分析得出,流体混合区、气泡以及尖钉的发展与初始扰动有密切的关系,特别是在后期影响更为显著;混合区宽度的变化过程和尖钉相似,而气泡高度的变化基本上呈线性增长趋势,且受初始扰动的影响比较小,但是其构型却有明显差别;网格的影响也主要体现在对混合区、气泡和尖钉的构型上。

关键词:多介质流体动力学;Richtmyer-Meshkov不稳定性;流体混合区

中图分类号:O347;O354 **文献标识码**:A